Electrode Catalysis of the Four-Electron Reduction of Oxygen to Water by Dicobalt Face-to-Face Porphyrins

James P. Collman,*[1a] Peter Denisevich,[1a] Yutaka Konai,[1a] Matt Marrocco,[1a] Carl Koval,[1b] and Fred C. Anson*[1b]

Contribution from the Department of Chemistry, Stanford University, Stanford, California 94305, and the Division of Chemistry and Chemical Engineering, California Institute of Technology, Pasadena, California 91125.
Received December 10, 1979

Abstract: A series of dimeric metalloporphyrin molecules has been synthesized in which the two porphyrin rings are constrained to lie parallel to one another by two amide bridges of varying length that link the rings together. These cofacial metalloporphyrins have been applied to the surface of graphite electrodes and tested for catalytic activity toward the electroreduction of dioxygen to water in aqueous acidic electrolytes. All molecules tested exhibited some catalytic activity, but hydrogen peroxide rather than water was the chief reduction product. However, the dicobalt cofacial porphyrin linked by four-atom bridges produced a catalyzed reduction almost exclusively to water and at exceptionally positive potentials. Rotating ring–disk voltammetric measurements were employed to diagnose the electrode reaction pathway and a possible mechanism for the observed catalysis is suggested. The results seem to demonstrate the participation of two metal centers in controlling the course of a multiple-electron process.

Introduction

The development of an electrode material at which the rapid four-electron reduction of dioxygen to water proceeded at or near the reversible potential (+1.23 V vs. SHE) would constitute a major advance in fuel cell technology. Present (acid-electrolyte) oxygen cathodes employing platinum metal as the electrode catalyst are too expensive for widespread application and, moreover, produce useful current densities only at overpotentials of several hundred millivolts. Numerous workers have examined the use of macrocyclic transition metal complexes as oxygen reduction catalysts,[2a-c] but most seem to function only at rather negative potentials and to effect only a two-electron reduction of dioxygen to hydrogen peroxide. The stepwise reduction of dioxygen, first to hydrogen peroxide (E° = 0.68 V) and, subsequently, to water, is unsuitable if a fuel cell cathode is to operate near 1.23 V. At this potential, the equilibrium concentration of H_2O_2 is only ca. 10^{-18} M; so to pass desirable current densities (say, 1.0 A cm^{-2}) via a stepwise reduction would require a standard heterogeneous rate constant for the reduction of hydrogen peroxide to water greater than 10^{12} cm s^{-1}. This value far exceeds the collision-limited rate ($\sim 10^4$ cm s^{-1}). If the hydrogen peroxide were to be consumed by disproportionation to dioxygen and water, the rate constant for this reaction would have to be near 10^{22} M^{-1} s^{-1}. Clearly, the intermediacy of hydrogen peroxide in an overall four-electron reduction of oxygen is impractical for fuel cell applications at potentials near 1.23 V.

In designing possible oxygen reduction catalysts, we look, therefore, for materials capable of delivering four electrons, more or less simultaneously, to the dioxygen substrate at as positive a potential as possible. A mononuclear complex is highly unlikely to effect such a reduction in a rapid fashion, given the demands for spin, ligand, and solvent shell reorganization concomitant with a transfer of four electrons. We are thus led to the preparation of binucleating ligands, capable of holding two metal centers in a suitable geometry so that they may jointly bind a dioxygen molecule and, each metal center transferring two electrons, carry out the four-electron process. To this end, we have prepared a variety of porphyrin dimers linked so that the planar macrocycles and their metals are held in a "face-to-face" orientation. The interplanar separation of these dimers is designed to span distances of ca. 7–4 Å, including the ranges suggested by models for the proposed dioxygen complexes and intermediate μ-peroxo species. We have previously reported the preparation of some of these dimers;[2d] their application to the multielectron reduction of nitrous oxide is detailed elsewhere.[3] Other workers[4] have reported the synthesis and properties of related porphyrin dimer systems, including effects on the binding of dioxygen. Here, we discuss the use of such binuclear complexes in the electrocatalytic reduction of dioxygen.

In studying oxygen reduction mediated by these complexes, we have made extensive use of the technique of rotating ring–disk voltammetry,[5] which permits the quantitative measurement of (unwanted) hydrogen peroxide production and allows discrimination between the formation of such peroxide as an intermediate or merely as a minor side product. The ring–disk electrode assembly (Figure 1) comprises a pyrolytic graphite disk with a concentric platinum ring. The porphyrin to be tested as a reduction catalyst is applied to the graphite disk by irreversible adsorption from a dilute dichloromethane solution.[6] As the assembly is rotated, fresh, oxygen-saturated electrolyte is drawn vertically toward the disk surface and ejected radially across the disk and ring. The disk potential is controlled by a potentiostat and the (disk) current–potential profile records the oxygen reduction process. At the same time, the ring is held at a potential (+1.4 V) where any hydrogen peroxide reaching it is rapidly oxidized to dioxygen but no other electrode reactions proceed. The ring current response thus monitors hydrogen peroxide production, and the ratio of disk to ring currents, normalized for the collection efficiency, N_0, of the ring,[5] defines the relative contributions of the four-electron and two-electron reduction processes. Moreover, possible contributions to the disk current arising from subsequent reactions of H_2O_2 (reduction to water or disproportionation to water and dioxygen) may be evaluated by examining the dependence of the current ratio on electrode rotation rate.[5] At higher rotation rates, H_2O_2 is removed from the disk surface before

(1) (a) Stanford University; (b) California Institute of Technology.
(2) (a) J. H. Zagal, R. K. Sen, and E. Yeager, *J. Electroanal. Chem.*, **83**, 207 (1977), and references cited therein. (b) H. Behret, W. Clauberg, and G. Sandstede, *Ber. Bunsenges. Phys. Chem.*, **81**, 54 (1977), and references cited therein. (c) A review of earlier work is available: H. Jahnke, M. Schonborn, and G. Zimmerman, *Top. Curr. Chem.*, **61**, 133 (1976). (d) J. P. Collman, C. M. Elliott, T. R. Halbert, and B. S. Tovrog, *Proc. Natl. Acad. Sci. U.S.A.*, **74**, 18 (1977).
(3) (a) J. P. Collman, M. Marrocco, M. L'Her, and C. M. Elliott, manuscript in prepartion; (b) M. Marrocco, Ph.D. Dissertation, Stanford University, 1980.
(4) (a) C. K. Chang, *J. Am. Chem. Soc.*, **99**, 2819 (1977); (b) *Adv. Chem. Ser.*, No. **173**, 162–177 (1979), and references cited therein; (c) N. E. Kagan, D. Mauzerall, and R. B. Merrifield, *J. Am. Chem. Soc.*, **99**, 5484 (1977); (d) H. Ogoshi, H. Sugimoto, and Z. Yoshida, *Tetrahedron Lett.*, 169 (1977).
(5) (a) W. J. Albery and M. L. Hitchman, "Ring-Disc Electrodes", Clarendon Press, Oxford, 1971; (b) H. R. Thirsk and J. A. Harrison, "A Guide to the Study of Electrode Kinetics", Academic Press, New York, 1972.
(6) A. P. Brown, C. Koval, and F. C. Anson, *J. Electroanal. Chem.*, **72**, 379 (1976); A. P. Brown and F. C. Anson, *ibid.*, **83**, 203 (1977).

0002-7863/80/1502-6027$01.00/0

further reaction can take place, resulting in an increased ring current and decreased disk current. Invariance of the current ratio with rotation rate indicates the H_2O_2 is formed only as a parallel product in dioxygen reduction, not as an intermediate.[7]

Synthesis

The precursor (monomer) porphyrins were prepared by Fischer's route from monopyrroles. The expeditious modification developed by Battersby[8] and Chang[4] dispenses with the isolation of dipyrrolic materials—the intermediate dipyrromethenes are prepared and coupled in situ to yield the porphyrins. After reesterification of the crude reaction product, the desired porphyrin diesters **1a** and **1b** were isolated in crystalline form in good yield.

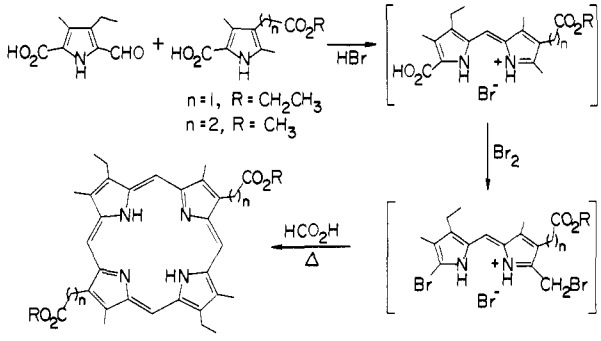

The diamine porphyrins required for the amide-linked dimers were obtained via Curtius degradations of the diesters. The diacetic and dipropionic esters **1a** and **1b** thus yielded the diamines **2a** and **2b** with two- and three-atom side chains, respectively. The hydrazinolysis of the porphyrin diesters proceeds readily in refluxing pyridine; however, light must be excluded during the reaction to avoid photoreduction of the porphyrins. The isolated porphyrin diamines are similarly light sensitive and were manipulated in subdued light.

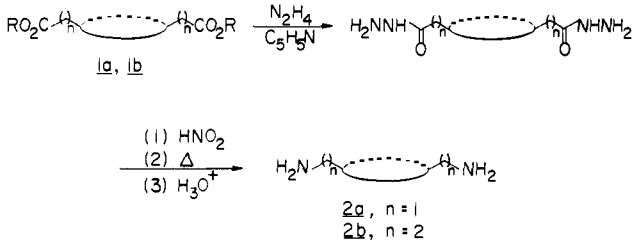

The *p*-nitrophenyl esters **3a** and **3b** offered stable, isolable, activated carboxylic acid derivatives, whose purity could be determined prior to the high-dilution condensation reaction forming the face-to-face dimers. Attempts to prepare acid chloride derivatives from the porphyrin diacetic acid were unsuccessful; oxalyl chloride was ineffective and thionyl chloride caused degradation of the porphyrin, perhaps as a result of meso chlorination.[9]

The nitrophenyl esters and diamines were coupled to form the face-to-face dimers under high-dilution conditions (0.5 mM). The most effective solvent was dry pyridine. The slow coupling reactions (ca. 8 h to reach completion) do not require the use of syringe pumps: equimolar amounts of the reactants were combined and the solution was heated at 50–70 °C until the reaction was complete. The products were readily isolated and purified by simple chromatography. By this method, the two nitrophenyl esters, **3a** and **3b**, and the two diamines, **2a** and **2b**, yielded the

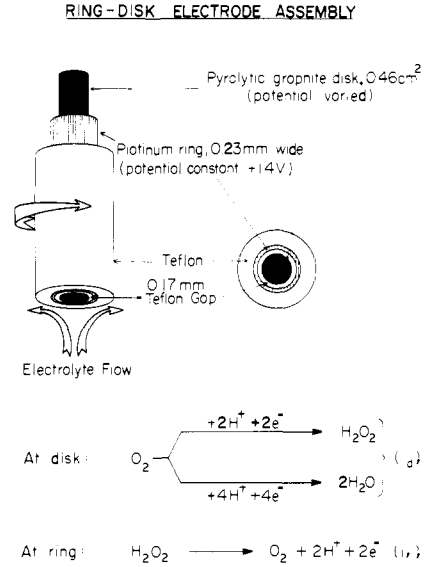

Figure 1. Schematic depiction of a rotating ring–disk electrode.

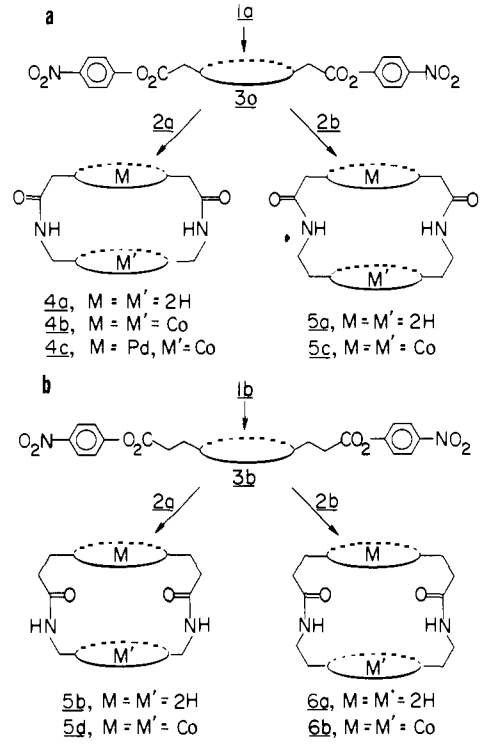

Figure 2. Scheme for preparing face-to-face porphyrins.

four face-to-face dimers with linking groups of six (**6**), five (**5a** and **5b**) (two isomers), and four (**4**) atoms (Figure 2). Examination of accurate molecular models indicates that these dimers represent interporphyrin distances of ca. 7 (six-atom linkages) to ca. 4 Å (four-atom linkages). Of course, possible molecular motions render such estimates ambiguous, particularly for the longer and more flexible linkages, but the range of interplane separations encompassed by this series of dimers includes the optimal hypothetical geometries for the binuclear oxygen reduction catalysts.

Dicobalt derivatives **4b**, **5c**, **5d**, and **6b** of the face-to-face dimers were prepared by the $CoCl_2$ method previously employed for the "picket-fence" compounds.[10] The "mixed-metal" dimer (PdCoFTF4, **4c**) containing cobalt and palladium was prepared by coupling the palladium complex of **3a** and the free-base diamine

(7) A. Damjanovic, M. A. Genshaw, and J. O'M. Bockris, *J. Chem. Phys.*, **45**, 4057 (1966).

(8) Professor A. Battersby kindly provided us, in advance of publication, with detailed directions for his expeditious synthesis of the bis(propionic acid) ester porphyrin **1b**. We extended this preparation to the bis(acetic acid) ester porphyrin **1a**. In the interim, Professor Battersby has independently prepared a similar series of cofacial porphyrin compounds.

(9) A. W. Johnson and D. Oldfield, *J. Chem. Soc. C*, 794 (1966).

(10) J. P. Collman, J. I. Brauman, K. M. Doxsee, T. R. Halbert, S. E. Hayes, and K. S. Suslick, *J. Am. Chem. Soc.*, **100**, 2761 (1978).

Table I. Representative ^{1}H NMR Data for Porphyrin Monomers and Dimers[a]

porphyrin	chemical shift, δ NH	CH_3 (ring)	CH_3 (ethyl)	H(meso)
	Monomers			
C2 diester 1a	−3.75	3.67	1.86	10.10, 10.16
C3 diester **1b**	−3.8	3.67	1.86	10.12, 10.05
Cl primary amine **2a**	−3.73	3.66	1.87	10.11, 10.16
C2 primary amine 2b	−3.75	3.65	1.87	10.09, 10.07
	Dimers			
FTF 6-3,2-NH **6a**	−6.1	3.51	1.68	9.0–9.4
FTF 5-3,1-NH **5b**	−8.2	3.60	1.62	8.7-8.9
FTF 5-2,2-NH **5a**	−7.90	3.55	1.65	8.7-8.9
FTF 4-2,1-NH **4a**	−8.1	3.60	1.60	3.7-8.9

[a] All spectra recorded at 100 MHz at room temperature in $CDCl_3$.

2a. Cobalt was then inserted in the dimer, as usual. The mild conditions of the coupling reaction should allow generalization of this approach to the preparation of a variety of mixed-metal complexes.

The palladium–cobalt dimer **4c** provides a test of the binuclear catalyst concept. Since the ligand environments of this species and the related dicobalt dimer **4b** (Co_2FTF4) are identical, any unusual reactivity of the latter complex must be due solely to the presence of two cobalt centers. Palladium should be an "innocent" metal center, as it shows no tendency to accept axial ligands, nor to participate in electron-transfer reactions.

NMR Spectroscopy

The ^{1}H NMR spectra of these dimers provide strong support for their face-to-face formulation (Table I). Particularly striking are the pronounced upfield shifts of the internal pyrrole NH protons, which are shielded by the ring current effects of the two porphyrins. Note that the internal pyrrole NH protons in the most closely spaced dimer, **4a**, have been shifted by 4.3 ppm compared with a monomer such as **1b**. The substituents on the porphyrin periphery and in the linking groups lie in the "blank" region of the shielding cone and are, therefore, less strongly shifted. These data are in good general agreement with those reported by Chang[5b] and again demonstrate that the pyrrole proton shifts are enhanced as the linking groups are shortened.

The NMR spectra of the face-to-face dimers provide inconclusive, but suggestive, data about the stereochemical nature of these compounds. As shown in Figure 3, the β-linked dimers can consist of two isomers, syn and anti, depending on the relative orientation of the two rings. A mixture of the two diastereomers can, in principle, show eight signals for the meso protons, since each diastereomer has two different meso hydrogens on each porphyrin ring. Thus, Chang has reported that his β-linked dimer with seven-atom linkages exhibits "seven weak signals" in the meso region, apparently resulting from a mixture of the isomers. The dimers prepared in the course of our work show only four quite well-resolved meso signals. The four-atom dimer, which is homogeneous according to thin layer chromatography, shows four meso signals, even in spectra recorded at 360 MHz.[11] However, high-pressure liquid chromatography of the free base **4a** reveals a major component and two faster moving, minor components. Each component exhibits the same electronic spectrum, including features which are associated with a cofacial orientation. The three components are not equilibrated upon heating for >6 h in boiling toluene. The relative amount of each component varies slightly from preparation to preparation. The gross mixture and the purified major component exhibit the same four meso hydrogen signals in their 360-MHz ^{1}H NMR spectra. The electrochemical

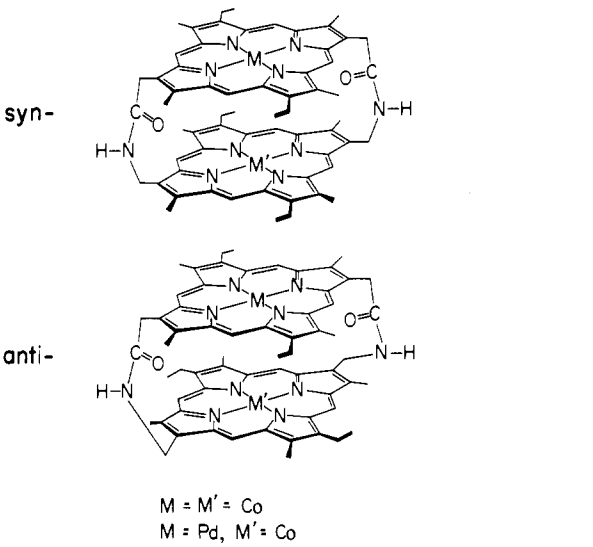

Figure 3. Syn and anti diastereomers of the β-linked face-to-face porphyrins. Other enantiomers are not shown. These structures are abbreviated: CO_2FTF 4-2,1-NH, indicating the metal derivative, a face-to-face porphyrin, the number of atoms linking the rings, the number of carbon atoms in the acid portion, the number of carbon atoms in the amine portion, and substitution on the N, respectively.

Table II. Selected ESR Parameters

	$g_\parallel$	$g_\perp$	$A_\parallel$[c]	$D_\parallel$[c]	$D_\perp$[c]
	Cobalt Complexes[a]				
Co C3 diester 1b	2.01	2.28	75		
Pd Co FTF 4-2, 1-NH **4c**	2.02	2.29	75		
Co_2 FTF 6-3, 2-NH **6b**		2.20	37	66	73
Co_2 FTF 5-3, 1-NH **5d**		2.28			153
Co_2 FTF 5-2, 2-NH **5c**		2.30			148
Co_2 FTF 4-2, 1-NH **4b**		2.28			171
	Copper Complexes[b]				
Cu octaethyl porphyrin	2.17	2.04	186		
Cu C3 diester	2.17	2.03	190		
Cu_2 FTF 4-2, 1-NH	2.17	2.01	101	405	387

[a] Spectra of cobalt complexes obtained in toluene–2-methyltetrahydrofuran glass (~100 K) in presence of ca. 30-fold excess of 1-methylimidazole. [b] Spectra of copper complexes obtained in dichloromethane glass (~110 K). [c] In units of 10^{-4} cm^{-1} (±10 × 10^{-4} cm^{-1}).

experiments described in this paper were performed on the gross mixture. Preliminary experiments indicate that the two minor components are even more active electrode catalysts than the major component. Studies of these substances are continuing.

Examination of molecular models suggests that the anti configuration minimizes steric interaction between substituents on the two rings (e.g., the ethyl groups are nearly "eclipsed" in the syn isomer). Since the formation of a syn or anti isomer is determined by the closure of the second amide linkage (assuming relatively free rotation of the two porphyrin rings after the first amide bond has been formed), such steric interactions could affect the resulting isomeric ratio. The mild, relatively slow nitrophenyl ester–amine coupling procedure may, in fact, promote the selective formation of the less encumbered anti isomer. Structural characterization of these compounds is still being investigated and will be reported in the future.

EPR Spectroscopy

Electron paramagnetic resonance spectroscopy was employed both in the characterization of the dicobalt dimers and as a means of monitoring their reaction with dioxygen. Selected EPR parameters are listed in Table II.

The dicobalt dimers exhibit spectra characteristic of exchange-coupled metal systems.[12] As shown in Figure 4, the

(11) We would like to thank the personnel at the Stanford Magnetic Resonance Laboratory for the 360-MHz spectra.

(12) G. Kokoszka and R. W. Duerst, *Coord. Chem. Rev.*, **5**, 209 (1970).

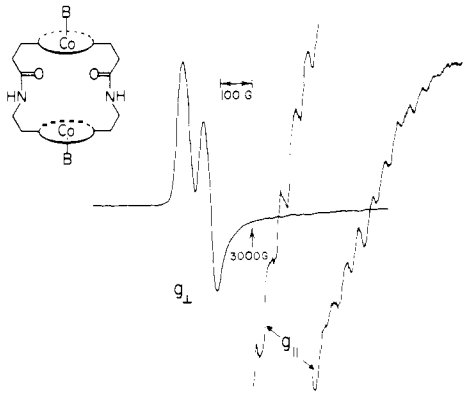

Figure 4. ESR spectrum (X-band) of Co_2FTF 6-3,2-NH·$(NMeIm)_2$.

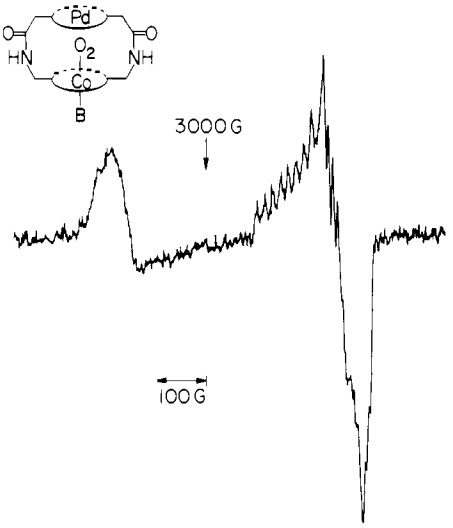

Figure 5. ESR of oxygenated Pd–Co dimer **4c**.

zero-field splitting (zfs) interaction of the two metal centers results in two transitions each for the "perpendicular" and "parallel" regions, the latter one further split by hyperfine coupling to the cobalt nuclei. In accord with simple theory, the hyperfine coupling constant $A_\parallel$ for the dimers is approximately one-half that of the corresponding monomeric species.

Although the magnitude of the zfs parameter, D (as estimated directly from the observed spectra), has been used to calculate metal–metal distances in simple systems,[2,4b,13] the spectra obtained for these dicobalt porphyrin dimers do not seem to permit such straightforward analysis. The estimated values for D (Table II) for dicobalt dimers **4b**, **5c**, and **5d** correspond to a metal–metal separation of ca. 6.5 Å, considerably larger than that indicated by molecular models. Even more distressing is the observation that D values for the dicopper complex of **4a** indicate a metal–metal separation of ca. 4.2 Å, more than 2 Å shorter than that of the analogous (and, presumably, isostructural) dicobalt species **4b**.

The meso-alkyl linked, face-to-face porphyrin dimers prepared by Collman and Schmittou[14] also gave EPR spectra exhibiting exchange coupling. For these species as well, the use of the EPR spectra to determine metal–metal distances was futile; estimates of D varied greatly for dicobalt and dicopper derivatives of the same dimeric ligand.

It seems apparent that the use of EPR spectra to determine metal–metal separation in these systems may require more sophisticated analysis. In particular, the simplifying assumption of coincident metal–metal and magnetic vectors remains unverified. Indeed, single-crystal X-ray diffraction studies of a meso-linked dimer (six-atom linkages) have shown the porphyrin rings to be severely displaced from coaxial geometry.[14] Such

(13) N. D. Chasteen and R. L. Belford, *Inorg. Chem.*, **9**, 169 (1970).

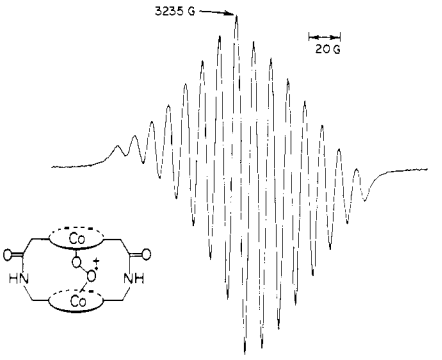

Figure 6. ESR of superoxo derivative of (Co_2FTF 4-2,1-NH), **4b**.

Table III. Ring–Disk Voltammetric Data

compd	$E_{1/2}$[a]	$i_r/i_d N_0$[b]	n[c]
Co C_2 diester	0.380	0.75	2.5
PdCo FTF 4-2, 1-NH	0.560	0.54	2.9
Co_2 FTF 6-3, 2-NH	0.515	0.52	3.0
Co_2 FTF 4-2, 1-NH	0.720	<0.067	>3.9

[a] Of catalyzed oxygen reduction wave, volts vs. NHE. [b] At $E_{1/2}$; N_0 is the ring collection efficiency.[5] [c] Calculated from $n = 4 - 2(i_r/i_d N_0)$.

displacements are expected to diminish the overall zfs interaction, but it is not clear why the dicobalt and dicopper chelates should act so differently. In addition, for the more closely linked dicobalt dimers, the possible contributions to zfs from orbital overlap and spin–orbit effects may be nonnegligible—the simple dipole–dipole model for zfs may not apply to these cases.

The EPR spectra of the oxygenated cobalt complexes are quite revealing. In the presence of a nitrogenous axial base, the cobalt complex of monomer **1a**, palladium–cobalt dimer **4b**, and the more widely spaced dicobalt dimer **6b** all gave spectra typical of 1:1 cobalt:O_2 adducts (e.g., Figure 5).[15] The more tightly linked dicobalt dimers **5c**, **5d**, and **4b**, on the other hand, rapidly yielded EPR-silent samples upon exposure to limited amounts of oxygen, presumably owing to formation of diamagnetic μ-peroxocobalt(III) species. Analogous results have recently been reported by Chang for similar face-to-face dicobalt porphyrin dimers.[16] As in Chang's case, these apparently diamagnetic complexes are readily oxidized by molecular iodine to give μ-superoxocobalt dimers, whose isotropic EPR spectra (Figure 6) are consistent with the presence of a single unpaired electron, localized on the superoxo bridge, and interacting equally with the two $I = {}^7/_2$ cobalt nuclei.[17]

It should be noted here that Chang's five-atom dimer contains *tertiary* amide linkages, whereas those employed in this work are linked with *secondary* amide groups. The rapid formation of the μ-peroxo species is thus not dependent upon the presence of an acidic NH proton, but rather upon the close proximity of the two cobalt centers. The marked contrast between the palladium–cobalt dimer **4c** and the dicobalt species **4b**, which have identical ligands, illustrates this point.

The meso-linked dicobalt dimers of Collman and Schmittou[14] showed no tendency to form bridging peroxo complexes under comparable conditions. Even for dimers with linking groups as short as four atoms, only spectra typical of 1:1 Co:O_2 adducts were obtained. Whether this results from a different electronic nature of the meso-substituted macrocycles or from a generally offset geometry of the two rings and metal centers remains unclear, but the latter seems more probable.

(14) (a) J. P. Collman, A. O. Chong, G. B. Jameson, R. T. Oakley, E. Rose, E. R. Schmittou, and J. A. Ibers, *J. Am. Chem. Soc.*, in press; (b) E. R. Schmittou, Ph.D. Dissertation, Stanford University, 1979.

(15) R. D. Jones, D. A. Summerville, and F. Basolo, *Chem. Rev.*, **79**, 142 (1979).

(16) C. K. Chang, *J. Chem. Soc., Chem. Commun.*, 800 (1977).

(17) (a) A. G. Sykes, *Prog. Inorg. Chem.*, **13**, 1 (1970); (b) J. A. Weil and J. K. Kinnaird, *J. Phys. Chem.*, **71**, 3341 (1967).

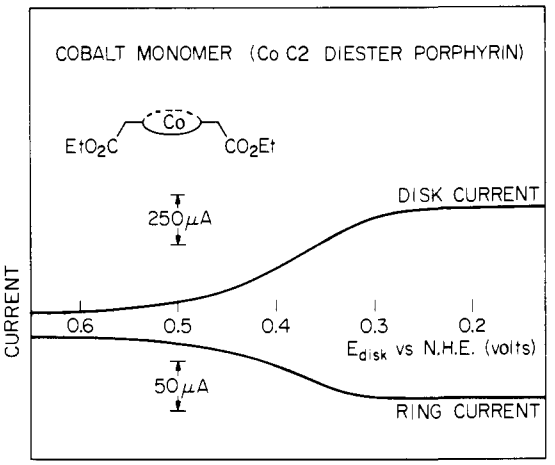

Figure 7. Disk and ring current vs. the potential of the graphite disk coated with the monomeric cobalt porphyrin shown. The platinum ring was maintained at +1.4 V. Rotation rate: 250 rpm. Supporting electrolyte: 0.5 M CF_3CO_2H saturated with oxygen at 1 atm.

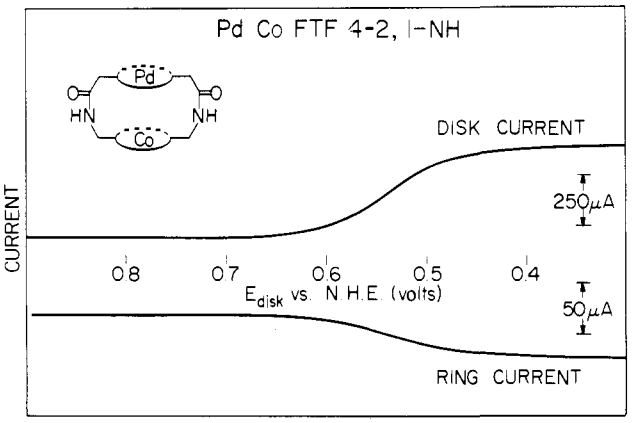

Figure 8. Disk and ring current vs. the potential of the graphite disk coated with the dimeric cobalt–palladium porphyrin shown. Other conditions as in Figure 7.

Electrochemistry

Typical ring–disk voltammetric results are shown in Figures 7–9 and the derived data are listed in Table III. All of the cobalt porphyrins catalyze the reduction of oxygen at graphite, but the potential at which reduction occurs, the magnitude of the disk current, and the amount of hydrogen peroxide detected vary markedly among the catalysts. At low rotation rate, the limiting disk currents increase linearly with the square root of the rotation rate, showing that the reduction current is limited by the rate of arrival of oxygen at the disk surface.[18] With the most active catalyst, **4b** (Figure 9b), the disk currents fall off the initially linear Levich plot of limiting current vs. (rotation rate)$^{1/2}$ at rotation rates greater than ca. 1000 rpm, and by 6000 rpm the current becomes essentially independent of rotation rate.

The monomeric cobalt porphyrin **1a** and the palladium cobalt dimer **4c** cause the reduction of oxygen to proceed primarily to hydrogen peroxide, a trait they share with cobalt phthalocyanines and related monomeric cobalt macrocycles.[2a-c] The dicobalt dimer **6b**, with six-atom linkages, also shows only monomer-like activity (Figure 9a). Dicobalt dimers with five-atom linkages, **5c** and **5d**, show somewhat greater activity in the form of increased disk currents and decreased ring currents, showing that a greater proportion of the oxygen is reduced directly to water.

For the most closely linked cobalt dimer, **4b**, however, the four-electron pathway is followed almost exclusively. The disk current at $E_{1/2}$ is almost twice as large as that in Figure 7 and very little hydrogen peroxide is detected at the ring (Figure 9b). The half-wave potential of the oxygen reduction wave is also considerably more positive for the most closely spaced catalyst, **4b**, although still considerably negative of the reversible potential.

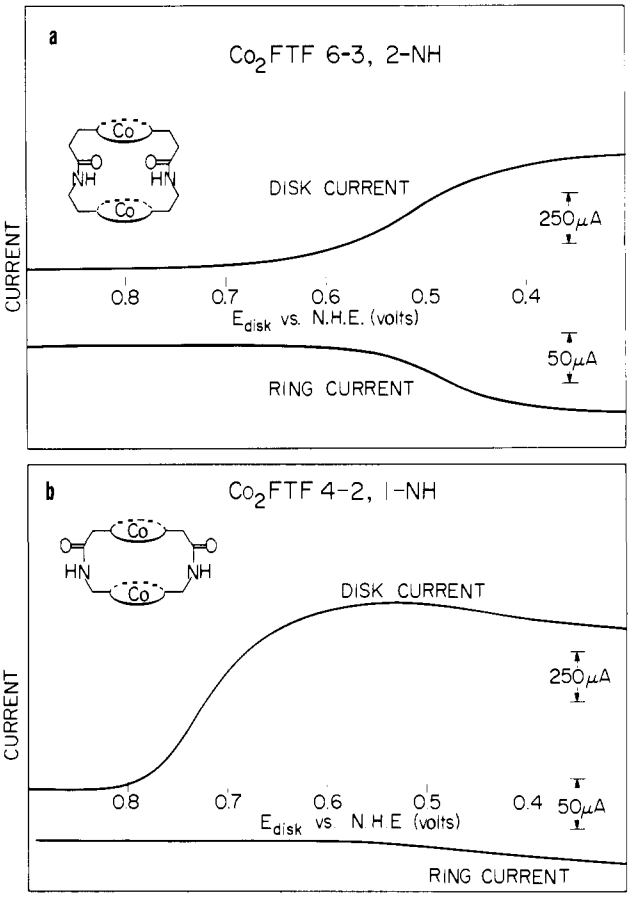

Figure 9. Disk and ring current vs. the potential of the graphite disk coated with the dimeric dicobalt porphyrins shown. Other conditions as in Figure 7.

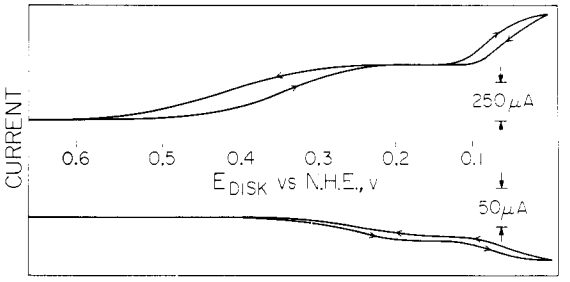

Figure 10. Disk and ring current vs. the potential of the graphite disk coated with the dicobalt porphyrin **4b**. Supporting electrolyte: 0.25 M $NaClO_4$, adjusted to pH 3.3 with $HClO_4$. Other conditions as in Figure 7.

Ring–disk experiments in oxygen-free electrolyte containing ca. 1 mM hydrogen peroxide established that none of the cobalt porphyrins catalyze the reduction or disproportionation of H_2O_2 within the potential range examined. Furthermore, the ratio of the disk-to-ring current did not depend on the electrode rotation rate, demonstrating that any hydrogen peroxide generated during oxygen reduction is stable to further reaction at the disk.[5,7] Thus, the production of hydrogen peroxide at the porphyrin-coated graphite appears to proceed in parallel with the four-electron reduction of oxygen to water.

The four-electron reduction process is strongly dependent on electrolyte pH. In (unbuffered) electrolytes in the range pH 3–4, two waves for oxygen reduction are observed (Figure 10). The current for the wave at more positive potentials, which produces

(18) V. G. Levich, "Physicochemical Hydrodynamics", Prentice-Hall, Englewood Cliffs, N.J., 1962.

(19) (a) R. H. Felton in "The Porphyrins", Vol. V, D. Dolphin, Ed., Academic Press, New York, Chapter 3; (b) D. G. Davis in ref 19a, Chapter 4; (c) A. Wohlberg, *Isr. J. Chem.*, **12**, 1031 (1974).

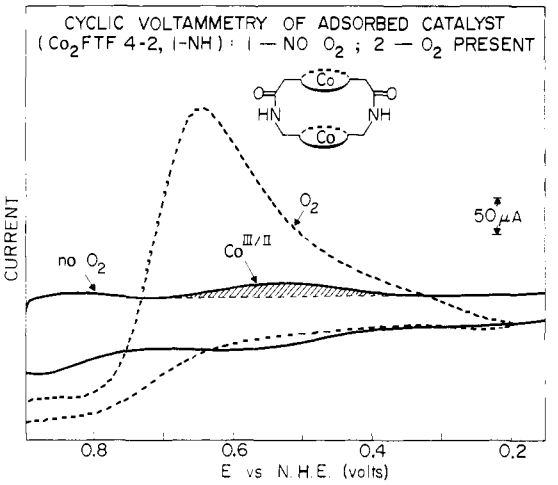

Figure 11. Cyclic voltammograms for a graphite electrode coated with dimer **4b** in the absence and presence of oxygen. Supporting electrolyte: 0.5 M CF_3CO_2H. Potential scan rate: 50 mV/s.

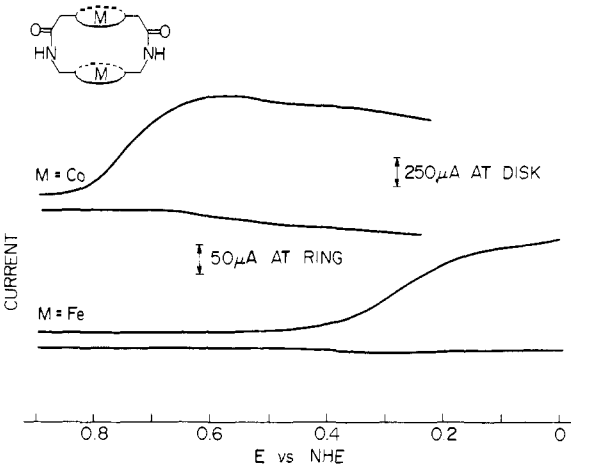

Figure 12. Disk and ring current vs. the potential of the graphite disk coated with **4b** or the diiron derivative of **4a**. Other conditions as in Figure 7.

little hydrogen peroxide, is limited by the supply of protons to the electrode surface: when the proton supply is depleted, the reduction process shifts to more negative potentials and hydrogen peroxide becomes a major product.

The pH dependence of this reduction process is in marked contrast to the results reported by Zagal et al.[2a] for oxygen reduction on electrodes coated with cobalt phthalocyanines. They observed hydrogen peroxide as the major reaction product in both acidic and alkaline electrolytes.

The onset of the oxygen reduction wave, catalyzed by the dicobalt dimer **4b**, corresponds to what we believe to be approximately the potential at which the second Co(III) in the dimer begins to be reduced to Co(II). A cyclic voltammogram of the catalyst adsorbed on the graphite disk in the absence of oxygen is shown in Figure 11. The foot of the small wave is close to the potential where the catalyzed reduction of oxygen commences in oxygen-saturated solutions (curve 2). Cyclic voltammetry of dimer **4b** in benzonitrile as solvent showed that the two cobalt(III) centers are reduced to cobalt(II) sequentially at potentials that lie ca. 200 mV apart.[20b] We presume that the same is true when the molecule is adsorbed on the electrode surface and that the small wave labeled $Co^{III/II}$ in Figure 11 corresponds to the reduction of the second Co^{III} center in dimer **4b** to Co^{II}. The wave for the reduction of the first Co^{III} center apparently is obscured by processes associated with oxidation and reduction of the graphite electrode itself. Thus, the observed behavior is consistent with the conversion of both cobalt centers in the catalyst to Co^{II} prior to the coordination and reduction of dioxygen. However, the nature of the oxidation state of the binary porphyrin catalyst is not firmly established. An alternative possibility is that only one cobalt has been reduced to the cobalt(II) state at the potential where oxygen reduction begins. In such a case, the other cobalt(III) center could have two roles in promoting an overall four-electron reduction. This cobalt(III) porphyrin should have a formal charge of 1+, which might cause the first cobalt(III/II) couple to occur at a more positive potential than that of a monomeric cobalt porphyrin complex. This cobalt(III) center could also serve as an adjacent Lewis acid, which might facilitate oxygen reduction by preventing the loss of hydrogen peroxide from the reaction site. At present, we consider this alternative to be less likely than the mechanism involving two cobalt(II) centers acting in concert on one dioxygen ligand. However, further experiments are necessary to clarify this point. Whichever mechanism is involved, it should be noted that in the most favorable case (Figure 9b) oxygen reduction begins at a more positive potential than the standard potential of the O_2/H_2O_2 couple (E = 0.68). At potentials significantly more positive than this value, thermodynamic considerations preclude the production of substantial quantities of hydrogen peroxide by any mechanism.

Tafel plots[5b] prepared from rotating disk current–potential curves at electrodes coated with dimer **4b** exhibited slopes that varied between ca. 70 and 90 mV/decade depending on electrode surface pretreatments. These values suggest a reaction whose rate is controlled by the concentration of a catalytic intermediate (e.g., the dicobalt(II) form of dimer **4b**) generated from the one-electron, quasi-reversible reduction of a precursor (e.g., the cobalt(II)–cobalt(III) form of **4b**). However, the presently available data are too sparse to support firm mechanistic conclusions.

The dimers with meso-alkyl linkages[14] show no remarkable catalytic activity: hydrogen peroxide is the major reduction product in all cases, even for the dicobalt dimer with four-atom linkages. As noted above, these meso-linked dimers do not display a joint action of the two metal centers in the binding of dioxygen—no peroxo-like species were formed. A further difficulty with these dimers is their more rapid loss of catalytic activity on the electrode—either the distorted (ruffled) macrocycles adhere more poorly to the graphite surface or the central metal ions are rapidly leached from these more basic ligands.

Results obtained for the diiron complex of the closely linked dimer **4a** are less dramatic (Figure 12). Although little hydrogen peroxide is detected at the ring, the potential of the oxygen reduction wave and the general shape of the disk and ring current–voltage profiles are almost identical with those of the monomeric iron analogues. Even monomeric iron porphyrins and phthalocyanines have been reported to mediate overall four-electron reduction of dioxygen, apparently via the formation and reduction or decomposition of hydrogen peroxide. The more negative potential at which the diiron complex catalyzes the reduction of oxygen in Figure 12 is in accord with the relative positions of the redox potentials of the $Fe^{III/II}$ and $Co^{III/II}$ monomeric porphyrin complexes.[19] Thus, for the systems examined here, no apparent benefit derives from the close proximity of two iron centers. Moreover, the iron complexes show a much more rapid loss of catalytic activity, reflecting, perhaps, the greater acid lability of the chelated ferrous ion or oxidative degradation of the porphyrin mediated by iron.

Catalyst Activation and Deactivation

The porphyrin-coated graphite electrodes show a gradual loss of catalytic activity during use: repetitive scans over the potential range 0.9–0.0 V display a decrease in both ring and disk current. Other workers have observed similar behavior with adsorbed porphyrins and phthalocyanines and were able to retard this degradation by incorporation of the catalyst species in the electrolyte.[2a] Unfortunately, the face-to-face dimers examined here are too insoluble in water to permit this remedy. We presume that this degradation represents the loss of catalyst from the

(20) (a) J. P. Collman, M. Marrocco, P. Denisevich, C. Koval, and F. C. Anson, *J. Electroanal. Chem.*, **101**, 117 (1979); (b) P. Denisevich, Ph.D. Dissertation, Stanford University, 1979.

electrode surface, since recoating the spent electrodes (without polishing) restores their activity, although usually incompletely. (Full polishing and readsorption, of course, restores full activity.) The probable cause of the catalyst attrition is chemical attack on the adsorbed porphyrin by peroxide or superoxide species rather than acid leaching of the chelated metal ion. Pretreatment of the catalytic electrode with acidic hydrogen peroxide solutions rapidly deactivates the catalyst, whereas pretreatment with aqueous acid reduces catalytic activity very slowly.

In an earlier preliminary report, we described an unusual hysteresis in the current–potential curves for the dicobalt dimer catalyst **4b**:[20] the half-wave potential for the initial scan toward more negative potentials was less positive than for the reverse and subsequent forward scans. We have subsequently determined that the presence of this hysteresis depends upon the extent of polishing of the graphite electrode surface prior to coating with the catalyst. With sufficiently heavy polishing, initial as well as subsequent current–potential curves appear at the same, more positive potential. This observation serves to emphasize the significant but, as yet, poorly understood role played by the graphite electrode surface in modulating the activity of attached catalysts. The surface of the polished graphite disk is probably intermediate between those in which the edges or the bases of the graphitic planes are exposed to the solution. The density of functional groups present on the polished electrode surfaces is probably much higher than that on a purely basal plane surface. It seems possible that functional groups on the graphite may serve as axial ligands to one of the centers in the dicobalt porphyrins. With some types of graphite electrodes the potentials where catalytic oxygen reduction proceeds are more negative than those shown in Figure 9b. This may be caused by differences in surface roughness and/or functional groups present on different types of graphite.

Proposed Mechanism

Although the data acquired thus far are insufficient to establish the mechanistic details of the oxygen reduction process, we can propose a sequence of steps consistent with the observed behavior.

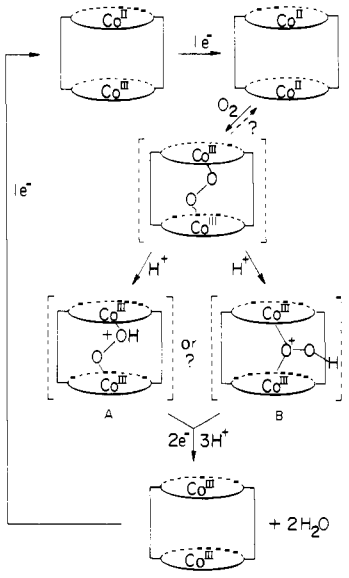

The reduction of the second of the two cobalt centers to the II oxidation state appears to commence very near to the potential at which the catalyzed oxygen reduction occurs. The coordination of oxygen by the effective catalysts seems a reasonable early step in the catalysis. We presume that the nickel and palladium complexes of the porphyrin monomers and dimers lack catalytic activity, at least in part, because they do not coordinate oxygen.

According to this scheme, rapid formation of the μ-peroxo intermediate is vital to the overall process. As seen in the EPR experiments, the more closely linked dicobalt dimers **5c**, **5d**, and **4b** are the only complexes examined capable of supporting this transformation. The electrocatalytic activity parallels this behavior. The much greater activity of dimer **4b** with the four-atom bridge may well reflect a more favorable conversion of a cobalt(II)–oxygen complex to the μ-peroxo form: if the oxygen complex is sufficiently long lived, it may be diverted into a pathway leading to hydrogen peroxide in the manner of the monomeric cobalt catalysts. The comparison of EPR and electrochemical results is, however, inexact, since the former experiments were conducted in the presence of a nitrogenous axial ligand, whereas the state of axial ligation of the graphite-bound catalyst remains uncertain. Strong donor ligands have been shown to increase the equilibrium binding of oxygen to cobalt porphyrins,[15] but their effect on the relatively slow (for monomeric porphyrins) formation of μ-peroxo dimers has yet to be clarified.

We attribute the strong pH dependence of the reduction process to a protonation of the peroxo bridge. The presence of positive charge on the peroxo bridge in the resulting cationic complex could facilitate electron transfer to the peroxo unit at more positive potentials than for the unprotonated precursor, with ultimate cleavage of the oxygen–oxygen bond.

An alternative version of this mechanism involves the formation of an end-bound hydroperoxy intermediate B, as shown. Similar species have been suggested as intermediates in the chemical reduction of simple μ-superoxo-dicobalt complexes in the presence of protons.[21] Although our data do not differentiate between the intermediacy of A and B, the shorter cobalt–cobalt distance required for the latter complex may account for the much higher catalytic activity of the most closely linked dimer **4b**. Similarly, the necessity of a hydroperoxy intermediate offers a rationalization for the inactivity of the meso-linked dimers: the offset geometry of these complexes may well interfere with formation of a species, such as B, that requires a coaxial orientation of the two metals. This special arrangement is impossible if the two porphyrin z axes are offset, as has been shown to be the case in at least one member of the meso-linked series.[14] The exquisite sensitivity of these catalysts to the geometry of these binary porphyrins is very significant and may be a general feature of such multielectron redox catalysts. It should be emphasized that our suggested mechanisms are still quite speculative. For example, we have not even established that the dioxygen substrate is reduced within the interporphyrin cavity. Nor, as mentioned earlier, are we certain that both cobalt centers are reduced to the II oxidation state before the catalytic reduction begins.

Recent work has shown that the μ-peroxo-bis(pentaammine)-cobalt(III) complex is quite resistant to reduction by homogeneous reductants.[21b] The complex decomposes into cobalt(II) and O_2 much more rapidly than it is reduced. However, porphyrin ligands used herein are quite different from ammonia.

The limiting disk current for the reduction of oxygen at electrodes coated with dimer **4b** achieves a maximum value of ca. 5 mA cm^{-2} at a rotation rate near 6000 rpm. It does not increase at higher rotation rates. We believe that this maximum current is determined by the rate of the reaction between dioxygen and the active, reduced form of the catalyst. We have not been able to obtain precise estimates of the quantity of catalyst present on coated electrodes but we believe that the catalyst is active when present in monolayer quantities. If a monolayer is assumed to include ca. 2×10^{-10} mol cm^{-2}, the 5 mA cm^{-2} maximum current corresponds to a molecular turnover number of ca. 60/s.

The high catalytic activity displayed by the tightly linked dicobalt dimer **4b** encourages us in the hope that still more effective oxygen-reduction catalysts may be prepared by simple modifications of this parent complex. Thus, it should be possible to shift the Co(III/II) redox potential to more anodic values by introducing electron-withdrawing groups (e.g., NO_2 or Cl) at the meso positions.[19c] To the extent that this redox couple governs the potential of oxygen reduction, such modified catalysts may function at more oxidizing potentials. A problem inherent in this sort of "tinkering" is the possibility that such electron-deficient complexes

(21) (a) M. R. Hyde and A. G. Sykes, *J. Chem. Soc., Dalton Trans.*, 1550 (1974). We thank Professor R. R. Gagné for suggesting this possibility to us. (b) M. Ferrer, T. D. Hand, and A. G. Sykes, *J. Chem. Soc., Chem. Commun.*, 14 (1980).

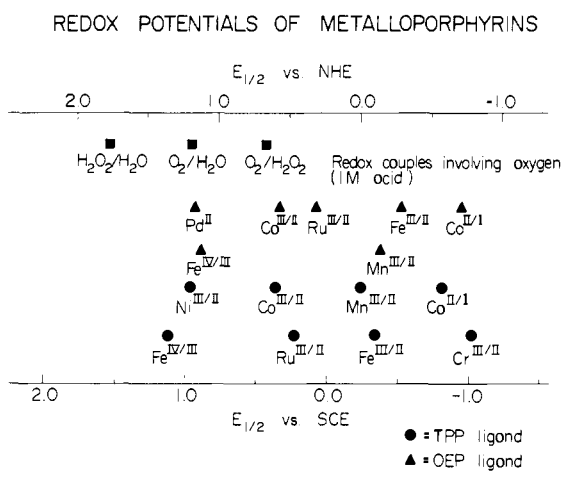

Figure 13. Redox potentials for various metal derivatives of *meso*-tetraphenylporphyrin and octaethylphorphyrin vs. normal hydrogen electrode. These values are taken from ref 19.

may show reduced oxygen affinities and, consequently, lower limiting current densities. Recent work has demonstrated the correlation between the Co(III/II) potential and equilibrium oxygen affinities for cobalt porphyrins and Schiff base complexes, the more easily oxidized species showing higher oxygen-binding constants.[15] Fortunately, rather small anodic shifts in the oxygen-reduction potential would be of great significance in fuel cell applications if the overall current densities can be maintained.

Prospects for creating more active catalysts by employing metals other than cobalt are not encouraging. As shown in Figure 13, the Co(III/II) couple is the most anodic of the (monomeric) metalloporphyrins with demonstrated affinities for oxygen. The ruthenium porphyrins appear at reasonably positive potentials and are, therefore, possible catalysts. The metalloporphyrins with highly anodic redox couples, such as Ni(III/II), Pd(II/IV?), and Fe(IV/III), show no tendency to bind oxygen, presumably because of their diminished electron availability.

We intend to investigate the effect of modifications of the linking groups on catalytic activity. It is apparent that, regardless of the actual mechanism by which these catalysts function, the process is extremely sensitive to the geometry of the dimers. Thus, the four-atom dimer is much more potent than the five- and six-atom dimers. The meso-linked dimers are uniformly monomer-like in behavior, regardless of chain length. As reported elsewhere,[3] one meso-linked dicobalt dimer is a highly effective catalyst for electrochemical reduction of nitrous oxide, whereas the β-linked species shows only modest activities toward this substrate. Again, a very specific geometry is apparently vital. Specific side-chain variations to be examined include the use of tertiary amide linkages: the amide NH protons may be involved in the overall oxygen reduction reaction, although, as mentioned before, such acidic protons are not required for μ-peroxo formation. The four-atom dimer with *amine* linkages has been prepared by reduction of the amide groups of **4a**.[22] Interestingly, its dicobalt derivative proved to be no more active as a catalyst than monomeric Co(II) porphyrins. Thus, protonation of the amine groups in the acid electrolyte employed appears not to facilitate proton transfer to the coordinated dioxygen. Nevertheless, a general synthesis of four-atom dimers with tertiary amide or amine linkages seems worth pursuing because such derivatives could provide a means of covalently attaching these species to graphite electrode surfaces and thereby increasing their durability as catalysts.

Experimental Section

Reagents and Solvents. All solvents and reagents were of reagent-grade quality, purchased commercially, and used without further purification, except as noted below or elsewhere. Benzene (thiophene-free), THF, and pyridine were refluxed with and distilled from CaH_2 under N_2. Toluene was distilled under N_2 from Na. DMF was distilled under reduced pressure from BaO onto Linde 4 Å molecular sieves. 2,6-Lutidine was purified by passage through an alumina column, followed by distillation from $BF_3{\cdot}Et_2O$. 1-Methylimidazole was vacuum distilled from KOH.

Silica gel for column chromatography was Type 62 (70–200 mesh), purchased from W. R. Grace. Alumina for column chromatography was Woelm neutral alumina (activity I). Alumina of activity III was prepared by adding H_2O to the activity I alumina. For TLC, commercially prepared silica and alumina plates from Analtech, Inc. were used.

Physical and Spectroscopic Methods. Melting points were obtained on a Mel-Temp Laboratory Devices capillary apparatus and are uncorrected. Electronic spectra were obtained on a Beckman DB-G or Cary 219 spectrometer. Only the Soret bands are listed. Note that all dimers show characteristic blue shifts of the Soret band.[2d,4b] Infrared spectra were recorded on a Perkin-Elmer 457 or Beckman Acculab 3 spectrometer. A Varian Instruments T-60 or Varian XL-100 was used for NMR spectra. Pulsed Fourier transform spectra were obtained on the XL-100 using a Nicolet Technology Corp. Model 1180 FT disk data system. Mass spectra were obtained on a Varian Instruments MAT 44 GC–MS system using the direct insertion mode, 70 eV ionization energy, and temperatures of 200–250 °C for porphyrin monomers. Dimers required temperatures of 300–350 °C to generate detectable molecular ion peaks. X-band ESR spectra were obtained on a Varian E-12 spectrometer. Elemental analyses were done by the Stanford Microanalytical Laboratory.

The ring–disk electrode (Figure 1), the electrode rotator, and the dual potentiostat were obtained from Pine Instrument Co., Grove City, Pa. The calculated collection efficiency of the electrode[5] was 0.18; the experimental value obtained by reducing ferricyanide at the disk was 0.17. To record current–potential curves, the disk potential was scanned at the rate of 5 mV/s. All potentials were measured vs. a SCE reference electrode but are reported vs. the standard hydrogen electrode (SHE).

Techniques for Handling Unstable Compounds. Some of the free-base porphyrins (the diamino and "face-to-face" porphyrins in particular) were found to be quite sensitive to light and/or oxygen, especially when dispersed on chromatographic plates or columns or in dilute solution. These compounds were manipulated in subdued light (no fluorescent illumination) and chromatographed in the dark (columns were also wrapped in aluminum foil). The Co(II) compounds were air sensitive (especially in the presence of axial ligands) and were prepared and purified in a Vacuum Atmospheres drybox with Mo-40 Dri-Train, capable of maintaining an atmosphere of N_2 with <1 ppm O_2 or H_2O. Spectra of these samples were obtained from cells or tubes closed with tightly fitting serum caps, which were lined with a thin film of silicone grease.

C3 Dimethyl Ester (1b).[26] To a solution of 3,5-dimethyl-4-methylcarboxyethylpyrrole-2-carboxylic acid[23] (5.625 g, 0.025 mol) and 5-formyl-4-ethyl-3-methylpyrrole-2-carboxylic acid[24] (4.525 g, 0.025 mol) in formic acid (20 mL) is added a solution of hydrogen bromide in acetic acid (12.5 mL of a 48% solution). After the mixture is stirred for 30 min, bromine (8 g, 0.05 mol) in formic acid (20 mL) is added and the mixture heated under reflux during 3 h. A loosely packed drying tube is fitted to the top of the condenser, as copious fumes of HBr are evolved. The mixture is cooled and evaporated to dryness on the rotary evaporator to produce a dark gum, to which methanol (50 mL) and concentrated sulfuric acid (0.5 mL) are added, and the mixture is stirred overnight (in the dark) to reesterify. The resulting solution is poured into water and the porphyrin extracted into chloroform. Separation of the organic phase and evaporation yield the crude product, which is dissolved in hot chloroform (40 mL) and hot methanol (40 mL). Upon cooling overnight in the refrigerator, the C3 porphyrin dimethyl ester separates in crystalline form (2.2 g, 29%).

The mother liquors from several preparations may be combined and passed through a short silica gel column, eluting with chloroform to remove tars. The eluates are evaporated and recrystallized from chloroform–methanol to yield additional pure porphyrin: mp 231–233 °C (lit.[25] 233 °C); NMR ($CDCl_3$) –4.0 (s, 2 H, NH), 1.8 (t, 6 H, CH_2CH_3), 3.18 (t, 4 H, CH_2CO_2), 3.55 (s, s, s, each 6 H, ring CH_3, ester CH_3), 4.0 (q, 4 H, CH_2CH_3), 4.26 (t, 4 H, $CH_2CH_2CO_2$), 9.9 ppm (s, s, 4 H, meso); λ_{max} 407 nm.

C2 Diethyl Ester (1a). The porphyrin condensation is conducted exactly as for the C3 ester above, on the same scale, using the pyrrole aldehyde acid and 3,5-dimethyl-4-ethylcarboxymethylpyrrole-2-carboxylic acid.[26] After evaporation of the formic–acetic acid mixture,

(22) K. Meier and J. P. Collman, to be published.

(23) A. R. Battersby, E. Hunt, E. McDonald, J. B. Paine III, and J. Saunders, *J. Chem. Soc., Perkin Trans. 1*, 1015 (1976).

(24) A. H. Jackson, G. W. Kenner, and D. Warburton, *J. Chem. Soc.*, 1328 (1965).

(25) H. Fischer and H. Orth, "Die Chemie des Pyrrols", Akademischer Verlag, Leipzig, 1937.

the residue is dissolved in absolute ethanol (100 mL) and concentrated sulfuric acid (3 mL) added. The mixture is allowed to stir in the dark during 3 days to reesterify, during which time the majority of the porphyrin ester crystallizes. The crystals are filtered off, washed with ethanol, and air dried. The product may be recrystallized from toluene in a Soxhlet apparatus, taking care to exclude air and light during the prolonged (ca. 48 h) extraction. In a few cases, the porphyrin ester did not separate out during the esterification procedure. If so, the ethanol was removed on the rotary evaporator and the residue taken up in chloroform and washed with a *small* amount of dilute ammonia. The tarry byproducts were removed on silica gel as above and the product was crystallized from chloroform–ethanol to yield 1.6 g (20%): NMR ($CDCl_3$) −3.75 (s, 2 H, NH), 1.22 (t, 6 H, ester CH_2CH_3), 1.8 (t, 6 H, ring CH_2CH_3), 3.55 (s, s, 12 H, CH_3), 4.2 (m, 8 H, CH_2CH_3, s), 5.01 (s, 4 H, CH_2CO_2), 10.1 ppm (s, s, 4 H, meso); mp 310 °C; *m/e* 594 (M^+, 100%); λ_{max} 406 nm. Anal. Calcd for $C_{36}H_{42}N_4O_4$: C, 72.8; H, 7.3; N, 9.3. Found: C, 72.1; H, 7.1; N, 9.2.

Curtius Rearrangements. C2 Hydrazide. The porphyrin diester **1a** (0.5 g) is dissolved with heating in 100 mL of dry pyridine. After solution is complete, 5 mL of anhydrous hydrazine is added and the solution heated at reflux, with total exclusion of light and air, during 36 h. At this point, the majority of the hydrazide has precipitated from the reaction mixture. The solution is cooled overnight in the refrigerator and filtered, and the hydrazide washed with methanol to yield 400 mg (85%) as a microcrystalline, red solid. Additional material may be recovered by dilution of the pyridine–methanol filtrates with water. IR: ν_{CO} 1650 cm^{-1} (broad). No (sharp) ester carbonyl at 1730 cm^{-1} should be present.

C1 Amine (2a). The above hydrazide (200 mg) is dissolved in 100 mL of acetic acid and 10 mL of 3 N HCl added. The solution is cooled to 0–5 °C (thermometer in mixture) and 3 mL of saturated sodium nitrite solution is added dropwise, with good stirring. The resulting red-brown solution is kept at 0–5 °C during another 10 min. Saturated sodium acetate solution (40 mL) is added and the azide extracted into dichloromethane (about 300 mL will be required). The organic phase is washed with ice-cold water, then with cold, saturated sodium bicarbonate solution, and dried over sodium sulfate. The solvent is removed on the rotary evaporator at room temperature. IR: ν_{N_3} 2130, ν_{CO} 1710 cm^{-1} (a small band at 2250 cm^{-1}, corresponding to the isocyanate, is usually present).

The crude azide is dissolved in 100 mL of dry toluene and heated at reflux during 2 h under nitrogen. The diisocyanate need not be isolated at this point—proceed then to the hydrolysis. If solid isocyanate is desired, the solvent may be removed in vacuo to give the diisocyanate as a crystalline solid. IR: ν_{NCO} 2250 cm^{-1}, no significant bands in the region 2000–1600 cm^{-1}.

To the solution of the isocyanate is added 100 mL of 3 N HCl and the mixture heated at reflux with good stirring during 3 h. After cooling, the aqueous layer is separated from the (colorless!) organic phase and washed with further toluene. Evaporation of the aqueous solution on the rotary evaporator (caution—foaming) gives the crude amine salt, which is taken up in methanol (100 mL). The solution is made strongly basic with NH_4OH and the diamine extracted into CH_2Cl_2. After drying over potassium carbonate, the amine is chromatographed on silica using $CHCl_3$–MeOH–Et_3N (95:5:0.5) as eluant. A small leading band is discarded and the diamine collected. The product may be crystallized from $CHCl_3$–MeOH containing a trace of ammonium hydroxide: yield 130–160 mg (60–80% from the hydrazide); NMR ($CDCl_3$) −3.73 (s, 2 H, NH), 1.87 (t, 6 H, CH_2CH_3), 3.65 (s, s, 12 H, ring CH_3), 4.1 (m, 4 H, CH_2CH_3), 5.25 (s, 4 H, CH_2NH_2), 10.12 ppm (s, s, 4 H, meso); λ_{max} 402 nm. Anal. Calcd for $C_{30}H_{36}N_6$: C, 74.8; H, 7.6; N, 17.5. Found: C, 73.9; H, 7.71; N, 17.1.

C3 hydrazide was prepared in identical manner from diester **1b** in 73% yield.

C2 amine (2b) was prepared from C3 hydrazide in same manner: yield 86%; NMR ($CDCl_3$) −3.75 (s, 2 H, NH), 1.87 (t, 6 H, CH_2CH_3), 3.66 (s, s, 12 H, ring CH_3), 4.2 (m, 12 H, CH_2), 10.1 (s, s, 4 H, meso); λ_{max} 401 nm. Anal. Calcd for $C_{32}H_{40}N_6$: C, 75.5; H, 7.9; N, 16.5. Found: C, 74.9; H, 7.75; N, 16.2.

Hydrolysis of Diesters. The appropriate diester (500 mg) is dissolved in CF_3COOH (20 mL) and concentrated HCl (5 mL) is added. The mixture is allowed to stand, stoppered, in the dark for 2 days. The solvents are removed in a nitrogen stream with gentle warming (water bath) to give a purple gum. HCl (6 N, 40 mL) is added and the mixture heated gently and triturated to reduce the gum to a microcrystalline powder. Cooling and filtration afford the porphyrin dicarboxylic acid (as the HCl salt) in essentially quantitative yield. NMR (pyridine-d_5) should reveal the absence of any esters. Note: the trifluoroacetic acid is employed to retain the porphyrins in solution during the course of the reaction. The use of HCl alone frequently results in the crystallization of incompletely hydrolyzed material, particularly in the case of **1a**. If free-base diacids are desired, they may be obtained by crystallization of the salts from pyridine–methanol, but this is not necessary for the preparation of the nitrophenyl ester below.

C3 Bis(nitrophenyl) Ester (3b). The C3 diacid (100 mg) is dissolved in 50 mL of dry pyridine and *p*-nitrophenyl trifluoroacetate[27] (200 mg) is added. The mixture is stirred at room temperature overnight with exclusion of light. The porphyrin ester gradually separates as red microcrystals. Hexane (100 mL) is added and, after several hours in the freezer, the product is filtered, washed with hexane until free from pyridine, and dried. TLC ($CHCl_3$) showed no material, except the desired diester (R_f 0.85): yield 110 mg (85%); IR ν_{CO} 1755, ν_{NO_2} 1520, 1340 cm^{-1}.

C2 bis(nitrophenyl) ester (3a) was prepared as for the C3 ester, in 88% yield.

Preparation of Face-to-Face Dimers. General Procedure for Coupling Diamines 2a and 2b with Nitrophenyl Esters 3a and 3b. The reactions are conducted in reagent-grade pyridine (stored over 4 Å molecular sieves) in an ordinary round-bottomed flask equipped with a magnetic stirrer and a short reflux condenser with nitrogen inlet. A water bath is convenient for maintaining the temperature at 55–70 °C. The nitrophenyl ester (0.02 mmol) is dissolved with slight heating in 100 mL of pyridine. As soon as dissolution is complete, the appropriate diamine (0.02 mmol), dissolved in 20 mL of pyridine, is added all at once. The reaction mixture is held at 55–70 °C, light being excluded. An insoluble polymer is gradually deposited. The progress of the reaction may be monitored by TLC (silica gel, $CHCl_3$–MeOH, 96:4), taking care to remove traces of pyridine. The reaction is generally complete after 8 h, at which time a small amount of diamine (R_f 0.1) may remain unconsumed; no nitrophenyl ester (R_f 0.9) should be present.

The pyridine is removed on the rotary evaporator and the residue dissolved in dichloromethane; the polymer will not dissolve. The solution is stirred briefly with a few milliliters of 0.5 M NaOH, washed with water to remove nitrophenol (yellow), and dried over K_2CO_3. Solutions of the dimers should be regarded as *highly light sensitive* and be handled in the dark. Chromatographic purification should be performed as expeditiously as possible, with complete exclusion of light. Additional notes for the individual dimers follow.

FTF 6-3,2-NH (6) is prepared from the C3 nitrophenyl ester **3b** and C2 diamine **2b**, and purified by preparative TLC (1000-μm silica plates) eluting with $CHCl_3$–MeOH (97:3). A small leading band is discarded and the product (R_f 0.4) collected: yield 35%, λ_{max} 384 nm; *m/e* 1039 (calcd, 1038).

FTF 5-3,1-NH (5a) is prepared from the C3 nitrophenyl ester **3b** and C1 diamine **2a**. Purification is as for **6**, again discarding the leading band: yield 36%, λ_{max} 380 nm; *m/e* 1011 (calcd, 1010).

FTF 5-2,2-NH (5b) is prepared from the C2 nitrophenyl ester **3a** and C2 diamine **2b**, using the same purification: yield 43%; λ_{max} 380 nm; *m/e* 1011 (calcd, 1010).

FTF 4-2,1-NH (4a) is prepared from the C2 nitrophenyl ester **3a** and C1 diamine **2a**. Preparative TLC purification is not necessary. The dichloromethane solution is rapidly chromatographed on a short silica column, eluting with $CHCl_3$–MeOH (96:4), to remove origin material and a trace of diamine. The product may be crystallized from hot toluene–chloroform: yield 55–60%; λ_{max} 375 nm; *m/e* 983 (calcd, 982). Anal. Calcd for $C_{62}H_{66}N_{10}O_2$: C, 75.4; H, 6.8; N, 14.1. Found: C, 73.9; H, 6.7; N, 13.1.

Pd(H_2) FTF 4-2,1-NH. Palladium was introduced into the C2 diester **1a** by the metal acetate method.[28] Mass spectroscopy indicated the absence of free-base prophyrin. Since this compound is totally insoluble in acid, the ester groups are cleaved as follows.

The palladium diester (250 mg) is dissolved with heating in 250 mL of pyridine. Ten milliliters of 2 N KOH and sufficient *i*-PrOH to render the mixture homogeneous (ca. 40 mL) are added. The resulting solution is heated at reflux under nitrogen overnight. The solvents are removed and the residue is dissolved in a small amount of water, filtering, if necessary, to remove a small residue. The palladium diacid is then precipitated with concentrated HCl.

The nitrophenyl ester derivative was prepared as for the metal-free compound and coupled with the diamine as usual. The resulting monopalladium dimer has similar chromatographic properties to the free base, with slightly lower solubility. Mass spectroscopy may be used to demonstrate the absence of any metal-free dimer: *m/e* 1087, 1089 (calcd, 1086, 1088).

(26) A. W. Johnson, E. Markham, R. Price, and K. B. Shaw, *J. Chem. Soc.*, 4254 (1958).

(27) S. Sakakibara and N. Inukai, *Bull. Chem. Soc. Jpn.*, **37**, 1231 (1964).

(28) J.-H. Fuhrhop and K. M. Smith in "Porphyrins and Metalloporphyrins", K. M. Smith, Ed., American Elsevier, New York, 1975.

Copper Complexes. Copper derivatives were prepared by the metal acetate method.[28] A chloroform solution of the chelate was passed through a short column of activity III alumina to remove traces of copper salts.

Cobalt Complexes.[10] In the inert atmosphere box the free-base porphyrin was dissolved in warm toluene, adding THF, if necessary, for dissolution. A small excess of 2,6-lutidine was added, followed by a tenfold excess of a saturated solution of $CoCl_2$ (anhydrous) in THF. The solution was heated gently (about 60 °C) during 1 h. The visible spectrum should show no free-base bands at ca. 620 nm. The solvent was removed in vacuo and the residue dissolved in a minimum of toluene. (Adding THF and no more than 10% MeOH may help.) The resulting solution was chromatographed on neutral alumina (activity III), eluting with toluene–THF (5:1). The eluate (cobalt salts remain on the top of the column) was evaporated in vacuo to give the four-coordinate cobalt complex. For Co_2FTF-4,2,1-NH (**4b**), *m/e* 1096, 1097 (calcd, 1096).

Acknowledgments. This work derives from a collaborative effort which also includes the research groups of Professors M. Boudart and H. Taube (Stanford) and H. Tennent (Hercules Inc. Research Center). The analysis of the possible role of intermediates in the four-electron reduction of oxygen at 1.23 V was first developed by Taube and Tennent. We owe a debt to Professor A. Battersby for the synthesis of the substituted porphyrins (see ref 8). We acknowledge K. Meier and J. Sessler for clarifying the hysteresis effects at graphite electrodes and for assistance with electrochemical studies. T. Geiger contributed many helpful suggestions and recorded Figure 7. E. Evitt, R. Pettman, and S. Bencosme prepared additional samples and examined the purification of **4b**. This work was supported by the National Science Foundation, Grants CHE78-08716, CHE78-09443, and CHE77-22722, by Grant GP23633 (Magnetic Resonance Laboratory), by the National Institutes of Health, Grant GM17880, and by the Stanford Institute for Energy Studies.

Polyarsenide Anions. Synthesis and Structure of a Salt Containing the Undecaarsenide(3-) Ion

Claude H. E. Belin

Contribution from the Laboratoire des Acides Minéraux, Laboratoire associé au CNRS No. 79, Université des Sciences et Techniques du Languedoc, 34060 Montpellier, France.
Received February 15, 1980

Abstract: Reaction of solid KAs_2 with 2,2,2-crypt (4,7,13,16,21,24-hexaoxa-1,10-diazobicyclo[8.8.8]hexacosane) in ethylenediamine yields deep-red rods which have been shown to be (crypt-K^+)$_3As_{11}^{3-}$ by X-ray crsytallography. The compound crystallizes in the $P\bar{1}$ space group with $Z = 2$ and $a = 14.248$ (4) Å, $b = 23.480$ (3) Å, $c = 14.015$ (4) Å, $\alpha = 99.17$ (2)°, $\beta = 101.60$ (2)°, and $\gamma = 98.24$ (2)° at 25 °C. Diffraction data were measured over four octants using an automatic Nonius CAD4 diffractometer and monochromated Mo Kα radiation. The structure was solved by direct methods. The full-matrix, least-squares method refined the structure to $R = 0.112$ and $R_w = 0.142$ from 4521 independent reflections with anisotropic temperature factors for arsenic and potassium atoms and isotropic temperature factors for light atoms. The main feature of the structure is the existence of the As_{11}^{3-} anion displaying an unusual geometry; its configuration is very close to the ideal D_3. Eight arsenic atoms are tricoordinated and arranged on a bicapped twisted triangular antiprism; the structure is achieved by three bridging waist arsenic atoms which are bicoordinated. According to Wade's theory, the geometry of the anion clearly derives from a 17-vertices polyhedron basis.

Introduction

Electrochemical studies of Zintl and co-workers[1] on sodium–arsenic alloys in liquid ammonia served to identify homopolyatomic anions As_3^{3-}, As_5^{3-}, and As_7^{3-}. Although As_7^{3-} is reported in crystalline Ba_3As_{14},[2] any attempt to isolate other solid derivatives of Zintl anions has been generally fruitless since the only new solid products obtained by evaporation of NH_3 from the solutions were amorphous and reverted to the known alloy phases.

The other works reported on potassium or sodium polyarsenides are from Hugot,[3,4] Lebeau,[5] and Dorn and co-workers.[6] Hugot prepared the red compound $K_2As_4 \cdot NH_3$ by directly reacting potassium with an excess of arsenic in liquid NH_3. More recently, Dorn investigated the system K–As using thermal analysis up to 60 atom % As and X-ray methods for As-richer regions. He found the compounds K_3As, K_5As_4, KAs, and KAs_2, the latter being described as a red compound that sublimes without decomposition and is similar to Hugot's compound.

Recently, a general way to stabilize homopolyatomic anions was found by Corbett and co-workers.[7] They used the bicyclic 2,2,2-crypt[8] to complex the sodium or potassium counterion and prevent electron transfer back to the cation and reversion to the known alloy phase. This procedure has now allowed the isolation and characterization of the stable homopolyatomic anions such as Sn_9^{4-},[9,10] Pb_5^{2-} and Sn_5^{2-},[11] Sb_7^{3-},[12] Te_3^{2-},[13] Ge_9^{4-} and Ge_9^{2-},[14] and Bi_4^{2-}.[15]

In the present work, we have studied reactions in liquid ammonia and ethylenediamine (en) of 2,2,2-crypt with either KAs_2 or $K_2As_4 \cdot NH_3$ compounds; the reaction schemes are different

(1) E. Zintl, J. Goubeau, and W. Dullenkopf, *Z. Phys. Chem., Abt. A*, **154**, 1 (1931).
(2) W. Schmettow and H. G. v. Schnering, *Angew. Chem.*, **89**, 895 (1977); *Agnew. Chem., Int. Ed. Engl.* **16**, 857 (1977).
(3) C. Hugot, *C. R. Hebd. Seances Acad. Sci.*, **127**, 553 (1898).
(4) C. Hugot, *C. R. Hebd. Seances Acad. Sci.*, **129**, 603 (1899).
(5) P. Lebeau, *C. R. Hebd. Seances Acad. Sci.*, **130**, 502 (1900)
(6) F. W. Dorn, W. Klemm, and S. Lohmeyer, *Z. Anorg. Allg. Chem.*, **309**, 204 (1961).
(7) J. D. Corbett, D. G. Adolphson, D. J. Merryman, P. A. Edwards, and F. J. Armatis, *J. Am. Chem. Soc.*, **97**, 6267 (1975).
(8) 4,7,13,16,21,24-Hexaoxa-1,10-diazobicyclo[8.8.8]hexacosane (N-$(C_2H_4OC_2H_4OC_2H_4)_3$N): B. Dietrich, J. M. Lehn, and J. P. Sauvage, *Tetrahedron Lett.*, 2885 (1969).
(9) J. D. Corbett and P. A. Edwards, *J. Am. Chem. Soc.*, **99**, 3313 (1977).
(10) J. D. Corbett and P. A. Edwards, *J. Chem. Soc, Chem. Commun.*, 984 (1975).
(11) P. A. Edwards and J. D. Corbett, *Inorg. Chem.*, **16**, 903 (1977).
(12) D. G. Adolphson, J. D. Corbett, and and D. J. Merryman, *J. Am. Chem. Soc.*, **98**, 7234 (1976).
(13) A. Cisar and J. D. Corbett, *Inorg. Chem.*, **16**, 632 (1977).
(14) C. H. E. Belin, J. D. Corbett, and A. Cisar, *J. Am. Chem. Soc.*, **99**, 7163 (1977).
(15) A. Cisar and J. D. Corbett, *Inorg. Chem.*, **16**, 2482 (1977).

0002-7863/80/1502-6036$01.00/0